A humidity sensor based on a singlemode-side polished multimode-singlemode (SSPMS) optical fibre structure coated with gelatin

Xianfan Wang, Gerald Farrell, Elfed Lewis, Ke Tian, Libo Yuan, and Pengfei Wang

***Abstract*—A novel relative humidity sensor based on a singlemode-side polished multimode-singlemode (SSPMS) fibre structure coated with gelatin material is reported. The sensing principle and fabrication method of the proposed sensor are presented. The experimental method is demonstrated to provide the optimum thickness of coating layers in order to achieve the highest sensitivity of 0.14 dB/%RH and a fast response time of 1000 ms for a given RH sensing range. The developed humidity fibre optic sensor based on a gelatin coating shows great potential for many applications such as industrial production, food processing and environmental monitoring.**

***Index Terms*—Gelatin coating, humidity sensor, side polished fibre**

I. Introduction

Fibre optic sensors have received significant attentions from researchers given their advantages compared to conventional sensors of immunity to electromagnetic fields, compact size, low weight and potential for long distance operation (point of measurement to point of interrogation instrumentation). A variety of fibre optic sensors incorporating microfabrication techniques have been recently developed for a wide range of applications including measurements of refractive index (chemical)[1], curvature (shape)[2], temperature[3], humidity[4] and gas concentration[5]. Among them, optical fibre humidity sensors are commonly required in many industrial application fields including air conditioning, production, food processing, human breath rate monitoring, paper and textile production. As a result to date many researchers have focused on the development of optical fibre based humidity sensors, for example, a polymer-coated fibre Bragg grating (FBG) relative humidity sensor[6], humidity sensors based on long period grating (LPG) technology[7], a fast response humidity sensor based on a sub-wavelength-diameter fibre taper coated with a gelatin film[8], and a PVA-coated photonic crystal fibre interferometer humidity sensor[9]. However, the high cost of interrogation and/or a complex fabrication processes has inhibited the development of these humidity sensors into commercially viable products. It is well established that a singlemode-multimode-singlemode (SMS) optical fibre structure as a sensor has unique merits such as ease of fabrication, high sensitivity and low-cost compared with other optical fibre structures[3, 10, 11]. However traditional SMS fibre structures display poor sensitivity to humidity, since the multimode fibre cladding prevents the evanescent wave from interacting with the surrounding environment. It is possible to use post processing to expose the multimode fibre core to the surrounding medium including methods based on tapering[12], misalignment[13], hydrofluoric acid etching[14] and side polishing. Considering a number of factors such as fabrication cost, safety during fabrication and the sensors mechanical strength, side polished SMS fibre structures offer a viable route to fabrication of a sensor.

In order to enhance the sensitivity of the humidity sensor, several humidity sensing materials have been previously investigated and applied as coated layers including polyvinyl alcohol (PVA)[15], agarose[16], gelatin[17], polyethylene oxide (PEO)[18] and carbon nanotubes[19]. When the surrounding humidity changes, the refractive index of these materials exhibit a corresponding variation, and hence the transmission of light through the structures is altered in a detectable way, allowing for sensing of humidity.

In this paper, the fabrication process for a singlemode-side polished multimode-singlemode fibre structure (SSPMS) is described in detail. The cross-sectional and longitudinal profiles of the structure were characterized by employing a scanning electron microscope (SEM). The influence of side polishing on the transmitted spectrum of SMS fibre structure and SSPMS fibre structure was simulated theoretically based on the beam

This work was supported by the 111 project (B13015) at the Harbin Engineering University, Key Program for International S&T Cooperation Projects of China under grant 2016YFE0126500, National Natural Science Foundation of China (NSFC) under grant 61575050, Key Program for Natural Science Foundation of Heilongjiang Province of China under grant ZD2016012, and by the Fundamental Research Funds of the Central University and the Harbin Engineering University,. (Corresponding author: Pengfei Wang)

X. Wang, G. Farrell, K. Tian, L. Yuan and P. Wang are with the Key Laboratory of In-fiber Integrated Optics of Ministry of Education, College of Science, Harbin Engineering University, Harbin 150001, China (e-mail: heuwangfan@hrbeu.edu.cn; gerald.farrell@dit.ie; ketian@hrbeu.edu.cn; lbyuan@vip.sina.com; pwang@hrbeu.edu.cn). P. Wang and G. Farrell are also with the Photonics Research Centre, Dublin Institute of Technology, Kevin Street, Dublin 8, Ireland (email: pengfei.wang@dit.ie; gerald.farrell@dit.ie).

E. Lewis is with the Optical Fibre Sensors Research Centre, Department of Electronic and Computer Engineering, University of Limerick, Limerick, Ireland (email: Elfed.lewis@ul.ie).

propagation method (BPM). Three separate fibre samples with different grades of coatings, no gelatin, three layers of gelatin and six layers of gelatin were investigated experimentally and compared over a range of humidity values for sensitivity and response times. Finally, a fibre optic relative humidity sensor based on an SSPMS fib re structure coated with three layers of gelatin was developed, which has a maximum sensitivity of 0.14 dB/%RH, and a response time of 1000 ms. Additionally, this sensor exhibits a relatively low temperature dependence of 0.006 dB/ºC, which enhances the accuracy and repeatability of the humidity measurement.

II. Theoretical Analysis

According to previous research[20, 21], for a traditional SMS fibre structure, the electric field distribution of the input SMF is assumed to be $E(r,0)$, the eigenmodes LP_{nm} of the MMF being excited when the light propagates along the MMF. Due to the cylindrically symmetrical characteristic of the MMF, only LP_{0m} modes can propagate within the MMF. In this paper, SMF28 (Corning Inc.) and ASF 105/125 (Thorlabs) fibres were used as SMF and MMF respectively. The core/cladding diameters of the SMF and MMF are 8.3/125 μm and 105/125 μm respectively, while the core/cladding refractive indices of SMF and MMF are 1.4504/1.4447 and 1.4446/1.4271 respectively. Employing the beam propagation method (BPM), the field amplitude distribution along the MMF was obtained as shown in Fig. 1. From this, it is clear that most of the light propagates along the MMF in the guided mode, rather than the evanescent mode, because of the complete MMF cladding confinement.

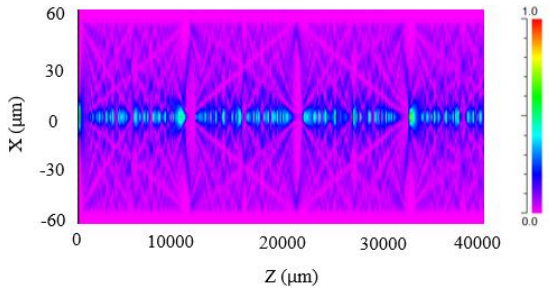

Fig. 1. Optical field amplitude distribution for light propagation along a standard MMF structure.

The SSPMS fibre structure used in this investigation is shown schematically in Fig. 2(a). The whole cladding and part of the core in the multimode fibre section are removed by polished to make the remaining fibre structure a D-shaped multimode waveguide, which allows the core section to be directly exposed to the external environment, providing the means for the required light-matter interaction. Figure 2(b) shows a vertical section of the SSPMS fibre structure, from which it can be seen that the SSPMS fibre structure consists of five sections when viewed from left to right: a lead-in SMF, a lead-in transitional section, the flat section, a lead-out transitional section and a lead-out SMF. The curved polished surface of the lead-in transitional section provides an efficient means to excite high-order modes and induces a strong evanescent field in the D-shaped multimode waveguide, which enhances its sensitivity to changes in the refractive index in the surrounding environment. The lead-out SMF collects the light from the side polished MMF flat section for output measurements. The geometrical parameters of the SSPMS fibre structure in the theoretical model are as follows: the side polished depth is 40 μm, the length of both the lead-in transitional section and lead-out transitional section is 2 mm, and the side polished MMF flat section has a length of 36 mm, which is sufficient to allow for useful evanescent field interaction with the external environment. Also, the transmitted intensity along the MMF core is attenuated, as illustrated in Fig. 2(c). By comparing Fig. 1 and Fig. 2. (c), we found that the light propagation pattern is altered significantly and more light power can interact with the surrounding environment when the MMF is side polished, which provides a potential capability for humidity sensing. The reason for this is that it is likely that increased optical power is transferred into the surrounding environment through evanescent field coupling which is effectively a loss in the transmitted power.

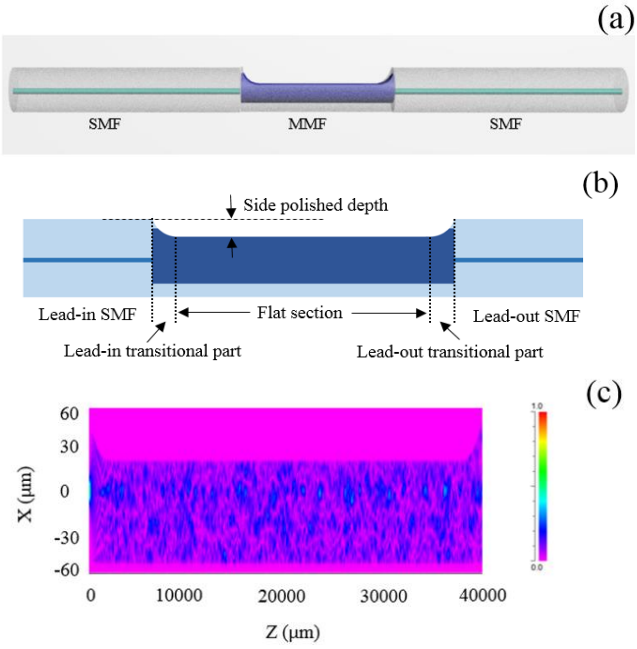

Fig. 2. (a) Schematic diagram of SSPMS fibre structure; (b) Schematic diagram of SSPMS fibre structure at vertical section; (c) Optical field amplitude distribution for light propagation along a SSPMS structure.

The operating principle for the humidity sensor of this investigation relies on the transmitted power loss referred to above and its variation with the value of the relative humidity of the external environment. The incident light of the fundamental mode propagates from the lead-in SMF, and high order modes are excited when the light enters the lead-in transitional part and side polished MMF flat section. It is well established that the evanescent field interaction increases with mode order[22]. Different propagation modes have different degrees of interaction through evanescent field coupling. The evanescent

This article has been accepted for publication in a future issue of this journal, but has not been fully edited. Content may change prior to final publication. Citation information: DOI 10.1109/JLT.2017.2730484, Journal of Lightwave Technology

field interaction increases with the mode order, thus higher order modes result in greater light-matter interaction in the environment immediately surrounding the fibre. In a side polished MMF, the effective mode number can be described as[23]

$$M = \frac{V_{SP-MMF}}{\pi} = \frac{2r}{\lambda}\sqrt{n_{co} - n_{ext}} \quad (1)$$

where r is the effective radius of the SP-MMF, n_{co} is the refractive index of the SP-MMF core and n_{ext} is the external refractive index. Therefore, when the refractive index of the external environment changes, the mode number M and the output spectral response will be changed accordingly[24]. Here, the Beam PROP simulation program (a part of the Rsoft Component Design Suite) was employed based on the beam propagation method (BPM). In the theoretical model both the lead-in and the lead-out curved polished transitional sections and the flat section of the D-shaped MMF fibre were simulated and the boundary condition of a perfectly matched layer (PML) is introduced to achieve a more accurate simulation result. The simulated results are illustrated in Fig. 3. From Fig. 3, the simulated relationship between transmission and wavelength is calculated over the wavelength range of 1500 nm – 1600 nm, for external refractive index values of 1.45 and 1.33. These two external refractive index values are chosen based on the known refractive index variation of the gelatin coating that occurs experimentally. From Fig. 3 it is evident that at a wavelength of 1558 nm for example, the value of the transmission loss decreases sharply when the external refractive index increases from 1.33 to 1.45.

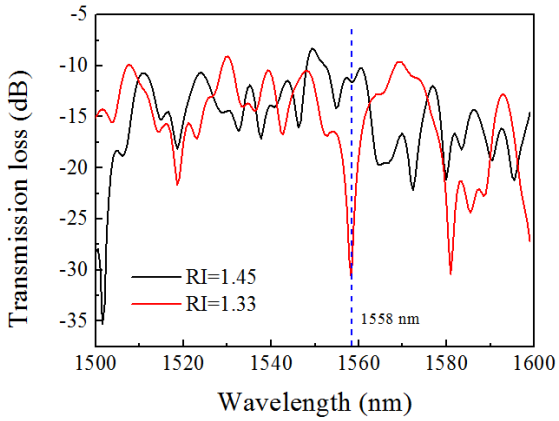

Fig. 3. Simulated optical spectrum of the SSPMS fibre structure with a side polished length of 4 cm and a side polished depth of 40 μm as the external refractive indices are 1.45 and 1.33.

III. Experimental Fabrication

As schematically depicted in Fig. 2 (a), the side polished SMS fibre structure comprises two identical singlemode fibres (SMF) and a side-polished multimode fibre (SP-MMF). Both SMFs and MMF have the same parameters of diameters (8.3/125 μm for SMF, 105/125 μm for MMF) and refractive index (1.4504/1.4447 for SMF, 1.4271/1.4446 for MMF) as used for the simulation part of Section 2 above. Firstly, a conventional SMS fibre structure was fabricated utilizing a high precision cleaver (Fujikura CT-32) and a commercial fusion splicer (Fujikura 62S) to sandwich a specific length of MMF between two SMFs. Then a fibre optic side polishing system was used to polish the SMS fibre as illustrated in Fig. 4. The two free ends of SMS fibre were fixed to two standing pulleys to keep the structure under tension. A rolling wheel overlaid with abrasive paper was designed for polishing the structure, which could freely roll back and forth utilizing a three dimensional mechanical adjustment. Additionally, different grades of abrasive papers with roughness of 6000, 8000, 10000-mesh were employed in sequence to ensure the smoothness of the finished side polished structure. In order to prevent or at least minimize the likelihood of fibre breakage, a 20g-weight was deployed which hung over fibre to balance tension during polishing as shown in Fig 4. The polished depth was monitored visually using a CCD linked to a PC, from which the captured MMF image was measured by a screen ruler, as depicted in the inset in Fig. 4.

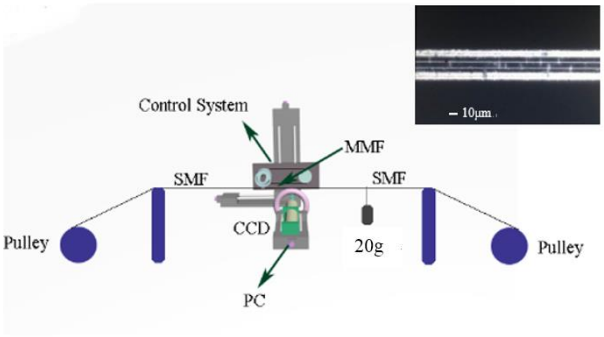

Fig. 4. Setup diagram for side polishing the SMS fibres, inset is the displayed side-polished MMF image on the screen of the PC.

The automatic polishing system allowed the polish time, depth and length to be pre-determined in a computer program so that the required polishing depth profile could be achieved. For the purpose of this investigation a 4 cm length polished region of the MMF was chosen, together with a 40 μm polish depth [25]. The influence of MMF length on the transmission spectra was investigated experimentally, and the results were shown in Fig. 5. It is found that the maximum extinction ratios are 25 dB, 28 dB, and 26 dB for MMF lengths of 3 cm, 4 cm and 5 cm respectively. It is well known that the dips with larger extinction ratios are more suitable for sensing as a result of providing an improved SNR. Additionally, previous studies [20] have shown a circa 4 cm length of fibre as an MMF section can give a reasonable multimode interference fringe over a measurable wavelength domain allowing a high sensitivity for a refractive index sensing measurement. Therefore a 4 cm length MMF was chosen for fabricating the sensors in these experiments. The influence of the polishing depth of MMF on the optical spectra was also investigated experimentally, with the results shown in Fig. 6. It is found that the maximum extinction ratios are 20 dB,

This article has been accepted for publication in a future issue of this journal, but has not been fully edited. Content may change prior to final publication. Citation information: DOI 10.1109/JLT.2017.2730484, Journal of Lightwave Technology

25 dB, and 19 dB for polishing depths of 30 μm, 40 μm and 50 μm respectively. It is well established that the dips with larger extinction ratios is more suitable for sensing as a result of its providing an improved SNR. This is the justification for choosing an SSPMS structure with a polishing depth of 40 μm as the experimental sample.

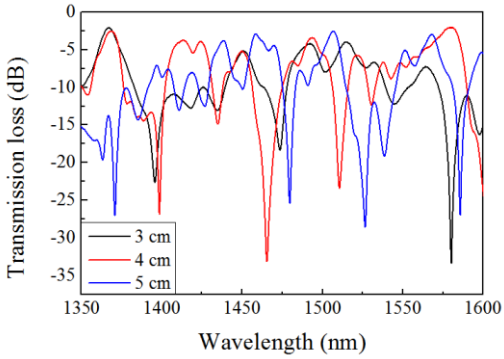

Fig. 5 Measured optical spectra of a SMS fibre structure with different MMF length of 3, 4, 5 cm.

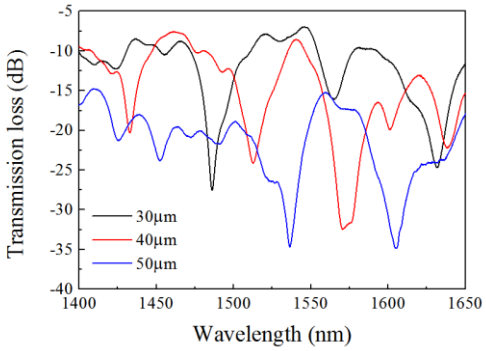

Fig. 6. Measured optical spectra of a SSPMS fibre structure with different polishing depth of 30, 40, 50 μm.

A minimal 20 μm polishing depth was chosen in the experiments due to the limited accuracy of the mechanical polishing system. After polishing the surface quality and side polish depth of the fabricated SSPMS fibres were confirmed experimentally using a scanning electron microscope (SEM). Fig. 7 (a) presents the microscope image of the top-view of the side-polished MMF section and Fig. 7 (b) and (c) represent the SEM images of the cross section of the MMF with side-polished depths of 20 μm and 40 μm respectively.

A Gelatin solution was prepared and coated on the modified SMS structure in order to enhance the humidity sensitivity of the SSPMS which also provided added mechanical strength to the structure. Gelatin (Ruibio, BoMei Co. Ltd) is a mixture of peptides and proteins, whose optical properties such as refractive index depend on the amount of water trapped in it[17]. The gelatin solution was prepared by dissolving gelatin powder in distilled water with a concentration of 5 % by weight. The solution was stirred at a temperature of 65 ºC until the gelatin powder was completely dissolved to form a homogeneous solution. The refractive index of gelatin solution in our experiments was measured as 1.3408 by using an Abbe refractometer (2WAJ). The gelatin solution was spin-coated on a glass slide and cured at room temperature for 24h. To obtain a uniform gelatin coating, a dip coating method was employed. The thickness of the coating was controlled by repeating the dip coating process several times, leading to the formation of several layers of gelatin.

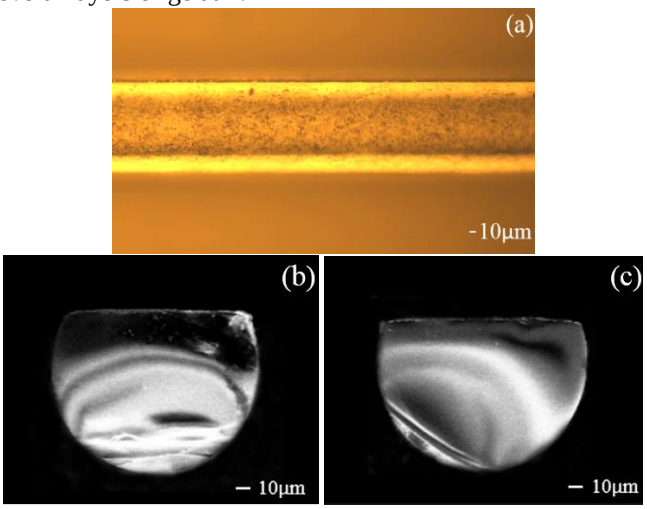

Fig. 7. (a) Zoom-in microscope image of the flat section of side polished MMF and the SEM images of the cross section of (b) 20 μm (c) 40 μm side-polished depth of SSPMS.

For the purpose of this investigation three separate samples were fabricated: a no gelatin coated SSPMS, three layers of gelatin coated on an SSPMS, and six layers of gelatin coated on an SSPMS. The three samples were designated as SSPMS 1, SSPMS 2 and SSPMS 3, respectively. The fabricated SSPMS fibres were left in a drying oven with an ultra-clean environment and a temperature of 25 ºC for 24 hours to allow complete moisture evaporation from the gelatin coating. After drying the new refractive index of the coating was measured as 1.474, since as the gelatin dries, its water content decreases and it is known that the refractive index of the gelatin increases when the water content in the coating decreases. Fig. 8 illustrates the experimental setup for the humidity sensing measurement of the fabricated SSPMS. The fibre samples were placed in a climate chamber (ESPEC SH-222), in which the temperature and humidity were controlled electronically, and values shown on an external display panel. A supercontinuum light source (YSL SC-series) was connected to the lead-in SMF to transmit a broad spectrum light signal to the SSPMS fibre structure, and the output response was monitored and recorded utilizing an optical spectrum analyzer (OSA) (YOKOGAWA AQ6370D). The output of the OSA was connected to and captured on a PC and stored in memory. To improve the repeatability of the results as well as enhancing the mechanical stability of the sensor setup, the fibre samples were fixed rigidly on a glass slide using a proprietary insulating kapton tape (Thorlabs KAP22-075) to eliminate unwanted fluctuations. The climate chamber was set to a constant temperature of 25 ºC, and the transmission spectrum under different humidity levels in the range 40 to 90 % RH were recorded using the OSA.

This article has been accepted for publication in a future issue of this journal, but has not been fully edited. Content may change prior to final publication. Citation information: DOI 10.1109/JLT.2017.2730484, Journal of Lightwave Technology

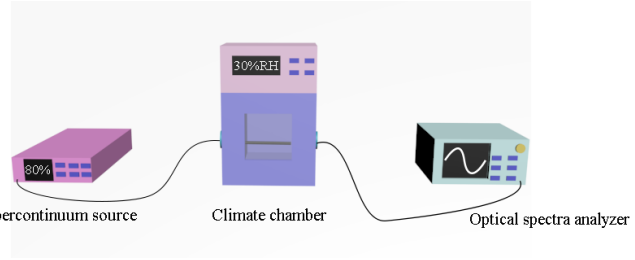

Fig. 8. Experimental setup for humidity measurement on an SSPMS fibre.

IV. Results and Discussion

The experimental results of spectral transmission loss for the SSPMS 1, SSPMS 2 and SSPMS 3 sensors are shown in Fig. 9. For SSPMS 1 (no coating), it is clear that as the humidity increases from 40% RH to 90% RH, the transmitted intensity in the 1490 -1515 nm wavelength range decreases as illustrated in Fig. 9 (a). The transmission loss in the center of the wavelength range increases (becomes more negative) by about -3.5 dB when the relative humidity changes 40%RH to 90%RH, The shift in the interference peak is a result of the adsorption and desorption of H_2O molecules along the rough surface of the side polished MMF, at the interface between air and silica glass [26]. In Fig. 9 (b), for SSPMS 2 (three layers of gelatin coating), the change in transmission loss was about -7.3 dB when the relative humidity was changed from 40 %RH to 90%RH. In Fig. 9 (c), for SSPMS 3 (six layers of gelatin coating), the transmission loss variation in the center of the wavelength range was about –19.5 dB within the humidity range 40 %RH to 90 %RH.

Fig.9 (d) shows the measured maximum transmission loss for each sensor in the wavelength range of interest as a result of varying the relative humidity value in the range 40% to 90%. Fig 9 (d) shows that a good linear correlation (R^2 = 0.994 for SSPMS 1, 0.880 for SSPMS 2, 0.985 for SSPMS 3) exists between the transmission loss and relative humidity for the three fabricated humidity sensors. It is also clear that the humidity sensitivity increases with increasing thickness of the gelatin coating. The sensitivities were measured as 0.07 dB/%RH, 0.14 dB/%RH and 0.38 dB/%RH for the sensors SSPMS 1, SSPMS 2 and SSPMS 3, respectively.

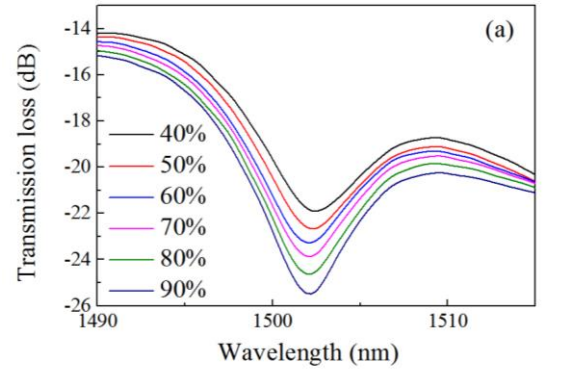

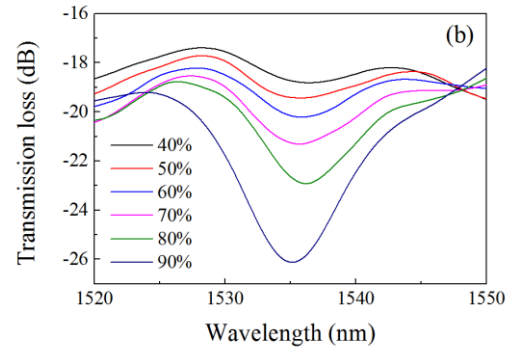

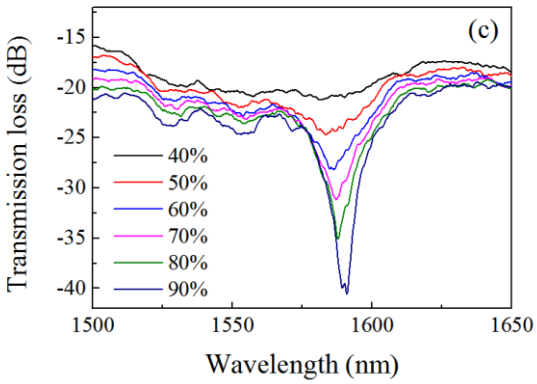

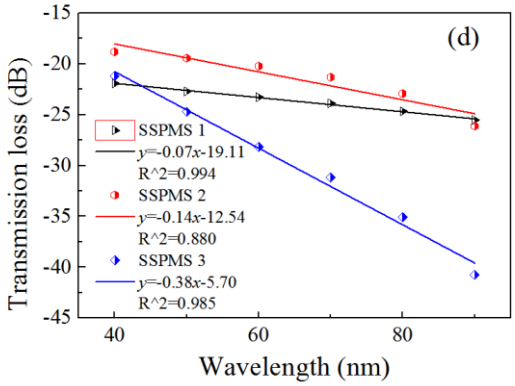

Fig. 9. Transmission spectral response of the samples of (a) SSPMS 1; (b) SSPMS 2; (c) SSPMS 3 with relative humidity variation; (d) relative humidity sensitivity of three fibre samples.

Additionally, it can also be observed from Fig. 9, that SSPMS 2 and SSPMS 3 coated with gelatin exhibit a deeper dip as relative humidity increases, the main reason for this being attributable to the refractive index of the gelatin being close to the value of the MMF core (1.4446) at the initial relative humidity, and the difference between the two values increases as the relative humidity increases. For SSPMS 3 (Fig 9(c)), the deterioration of the spectral signal is as a result of difficulty in providing a uniform gelatin coating on the 4 cm length of the side polished MMF when the thickness of the coating increases.

This article has been accepted for publication in a future issue of this journal, but has not been fully edited. Content may change prior to final publication. Citation information: DOI 10.1109/JLT.2017.2730484, Journal of Lightwave Technology

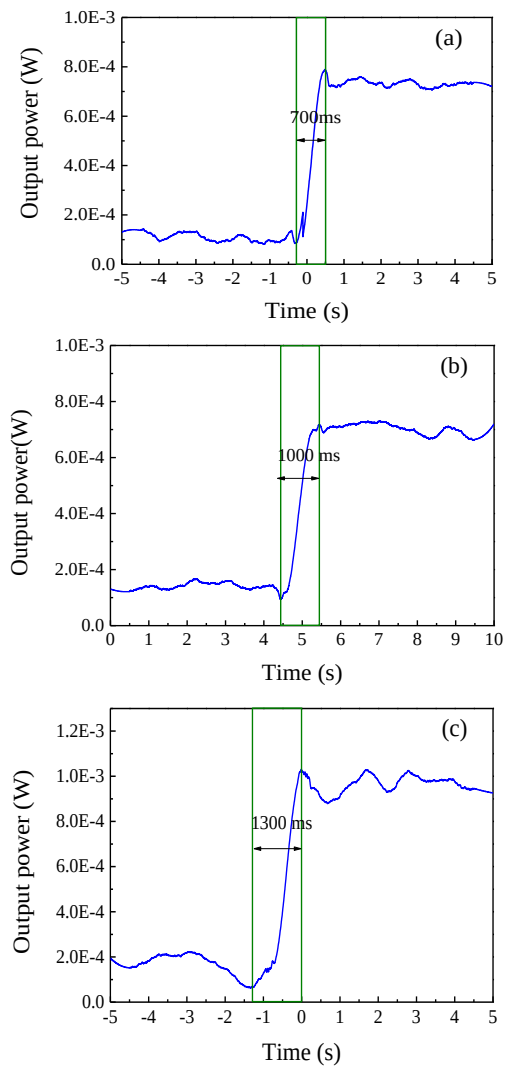

Fig. 10. Response time of the samples of (a) SSPMS 1; (b) SSPMS 2; (c) SSPMS 3, when the relative humidity changed from 90% to 40%.

In the case of humidity sensors it is also important to define the response time to the humidity variation. In this case, a photo-amplifier, oscilloscope (Tektronix MDO4034C) and tunable laser (Santec TSL-710) were used to measure the response time of the SSPMS 1, SSPMS 2 and SSPMS 3 sensors. The relative humidity was varied in a step manner from 90 %RH to an initial humidity (40 %RH) using the same environmental chamber as used in the experiments described above, and the output temporal optical intensity variation was recorded using the oscilloscope. Firstly, the relative humidity in the chamber was set at 90 %RH, and then the cover of the chamber was opened suddenly to expose the sensor to the environment of 40 %RH. Fig. 10 (a)-(c) show the resulting output optical power variation versus time of SSPMS 1, SSPMS 2 and SSPMS 3 when the input power was set to be 17 mW. If the response time is taken as being 0 to 100% change in value, they are respectively about 700 ms, 1000 ms and 1300 ms. These response times include the response time of the chamber itself. It is likely therefore that the actual sensor response times are faster. With an increase in gelatin coating thickness, the response time increase accordingly, since it takes a longer time for the adsorption and desorption of H_2O molecules within the gelatin coating layers.

TABLE I

SENSING PROPERTIES OF THE INVESTIGATED SSPMS 1, SSPMS 2 AND SSPMS 3

	HUMIDITY RANGE (%RH)	**Sensitivity (dB/%RH)**	**Response time (ms)**
SSPMS 1 (no gelatin coating)	40-90	0.07	700
SSPMS 2 (three layers of gelatin)	40-90	0.14	1000
SSPMS 3 (six layers of gelatin)	40-90	0.38	1300

The characteristics of the three optical fibre sensor samples: SSPMS 1, SSPMS 2 and SSPMS 3 are summarized in Table 1. Through comparison between the SSPMS 1, SSPMS 2 and SSPMS 3 samples and based on parameters listed in Table 1, it is evident that the SSPMS 3 has the highest sensitivity, while the SSPMS 1 sample has the fastest response time. Therefore which design is best suited for a particular application will depend on the needs of that application including sensitivity, rise time humidity range e.g.. If considering a simple tradeoff between sensitivity and time response, the SSPMS 2 sample may be the most suitable choice for the development of a general purpose humidity sensor as it has a response time of about 1000 ms and an average sensitivity of 0.14 dB/%RH. Its response time is 300 ms less than SSPMS 3 (six gelatin coatings), and its average sensitivity is twice as high as SSPMS 1 (no gelatin coating). On the other hand, from Fig.9 (c), it is clear that the thicker gelatin coated SSPMS is more vulnerable to producing an increasingly non-linear response as the gelatin coating thickness increases.

As with most optical fibre sensors, cross-sensitivity to temperature can be an important issue and in this study, it has been measured. Fig. 11 shows the variation in the measured spectral response of SSPMS 2, when the relative humidity was fixed at 40% RH, and temperature increased from 25 ^{o}C to 65 ^{o}C in the environmental chamber. From Fig. 11 it is clear that the influence of the temperature change results in a change of transmission loss. There exists a low temperature dependence of 0.006 dB/^{o}C within the temperature range of 25 ^{o}C-55 ^{o}C. However, beyond 65 ^{o}C, the transmission loss increases more rapidly with temperature because the gelatin coating begins to be dissolved. One advantage of the uncoated sensor is that, although it has the lowest sensitivity, it is not subject to the temperature limit circa 65 ^{o}C that the gelatin coated sensors are subject to. The results of Fig 11 indicate that the SSPMS 2 based humidity sensor has a relatively low temperature dependence in the range 25 ^{o}C to 55 ^{o}C and therefore has great potential for use in accurate monitoring of relative humidity.

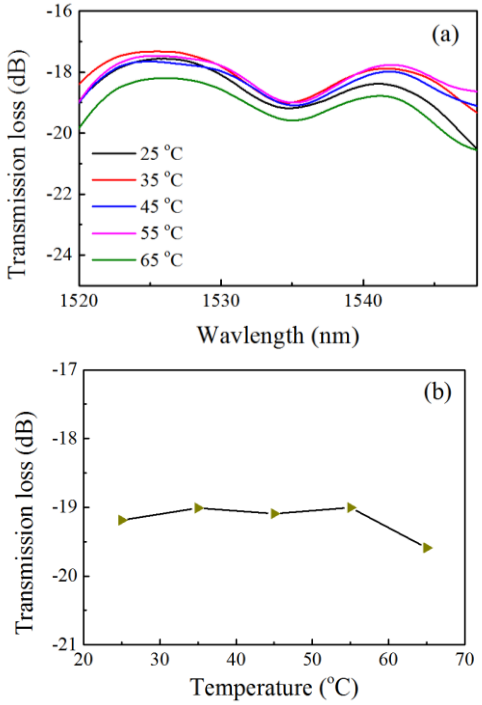

Fig.11. (a) Measured transmission spectrum shift with temperature range of 25 ºC-65ºC; (b) temperature dependence of SSPMS 2 fibre humidity sensor when 40% RH.

V. Conclusion

A novel optical fibre sensor based on a singlemode-side polished multimode-singlemode (SSPMS) structure has been successfully fabricated and characterized. The influence of side polishing on the transmitted optical spectrum and hence the sensor characteristic was simulated using the beam propagation method (BPM). A comparison of sensing performance using three different sensors with varying thickness of gelatin coating, has been conducted and demonstrated in an environmental chamber. The sensor exhibits an average sensitivity of 0.14 dB/ %RH within the humidity range 40 %RH- 90 %RH, and a relatively fast response time of 1000 ms. Additionally, its temperature dependence in the range 25 ºC to 65 ºC has been measured, and it exhibits a low temperature dependence of 0.006 dB/ºC within the temperature range 25 ºC to 55 ºC. The proposed gelatin coated SSPMS fibre sample can therefore be considered an excellent candidate as a general purpose environmental relative humidity sensor due to its low cost, operating range, ease of fabrication and fast response.

References

[1]P. F. Wang, G. Brambilla, M. Ding *et al.*, "High-sensitivity, evanescent field refractometric sensor based on a tapered, multimode fiber interference," *Optics Letters*, vol. 36, no. 12, pp. 2233-2235, Jun, 2011.

[2]K. Tian, Y. Xin, W. Yang *et al.*, "A curvature sensor based on twisted single-mode-multimode-single-mode hybrid optical fibre structure," *Journal of Lightwave Technology*, 2017.

[3]A. M. Hatta, G. Rajan, Y. Semenova *et al.*, "SMS fibre structure for temperature measurement using a simple intensity-based interrogation system," *Electronics Letters*, vol. 45, no. 21, pp. 1069-1070, Oct, 2009.

[4]J. L. An, Y. X. Jin, M. M. Sun *et al.*, "Relative Humidity Sensor Based on SMS Fiber Structure With Two Waist-Enlarged Tapers," *Ieee Sensors Journal*, vol. 14, no. 8, pp. 2683-2686, Aug, 2014.

[5]W. Jin, H. L. Ho, Y. C. Cao *et al.*, "Gas detection with micro- and nano-engineered optical fibers," *Optical Fiber Technology*, vol. 19, no. 6, pp. 741-759, Dec, 2013.

[6]T. L. Yeo, T. Sun, K. T. V. Grattan *et al.*, "Characterisation of a polymer-coated fibre Bragg grating sensor for relative humidity sensing," *Sensors and Actuators B-Chemical*, vol. 110, no. 1, pp. 148-155, Sep, 2005.

[7]T. Venugopalan, T. Sun, and K. T. V. Grattan, "Long period grating-based humidity sensor for potential structural health monitoring," *Sensors and Actuators a-Physical*, vol. 148, no. 1, pp. 57-62, Nov, 2008.

[8]L. Zhang, F. X. Gu, J. Y. Lou *et al.*, "Fast detection of humidity with a subwavelength-diameter fiber taper coated with gelatin film," *Optics Express*, vol. 16, no. 17, pp. 13349-13353, Aug, 2008.

[9]T. Li, X. Y. Dong, C. C. Chan *et al.*, "Humidity Sensor With a PVA-Coated Photonic Crystal Fiber Interferometer," *Ieee Sensors Journal*, vol. 13, no. 6, pp. 2214-2216, Jun, 2013.

[10] A. Kumar, R. K. Varshney, S. Antony *et al.*, "Transmission characteristics of SMS fiber optic sensor structures," *Optics Communications*, vol. 219, no. 1-6, pp. 215-219, Apr, 2003.

[11] P. F. Wang, G. Brambilla, M. Ding *et al.*, "Investigation of single-mode-multimode-single-mode and single-mode-tapered-multimode-single-mode fiber structures and their application for refractive index sensing," *Journal Of the Optical Society Of America B-Optical Physics*, vol. 28, no. 5, pp. 1180-1186, May, 2011.

[12] Y. Zhao, L. Cai, and H. F. Hu, "Fiber-Optic Refractive Index Sensor Based on Multi-Tapered SMS Fiber Structure," *Ieee Sensors Journal*, vol. 15, no. 11, pp. 6348-6353, Nov, 2015.

[13] A. M. Hatta, G. Farrell, P. Wang *et al.*, "Misalignment Limits for a Singlemode–Multimode–Singlemode Fiber-Based Edge Filter," *Journal of Lightwave Technology*, vol. 27, no. 13, pp. 2482-2488, 2009.

[14] Q. Wu, Y. Semenova, P. Wang *et al.*, "High sensitivity SMS fiber structure based refractometer--analysis and experiment," *Optics Express*, vol. 19, no. 9, pp. 7937-7944, 2011.

[15] A. Gaston, F. Perez, and J. Sevilla, "Optical fiber relative-humidity sensor with polyvinyl alcohol film," *Applied Optics*, vol. 43, no. 21, pp. 4127-4132, Jul, 2004.

[16] J. Mathew, Y. Semenova, and G. Farrell, "Effect of coating thickness on the sensitivity of a humidity sensor based on an Agarose coated photonic crystal fiber interferometer," *Optics Express*, vol. 21, no. 5, pp. 6313-6320, Mar, 2013.

[17] K. M. Tan, C. M. Tay, S. C. Tjin *et al.*, "High relative humidity measurements using gelatin coated long-period grating sensors," *Sensors and Actuators B-Chemical*, vol. 110, no. 2, pp. 335-341, Oct, 2005.

[18] J. Mathew, Y. Semenova, G. Rajan *et al.*, "Improving the sensitivity of a humidity sensor based on fiber bend coated with a hygroscopic coating," *Optics and Laser Technology*, vol. 43, no. 7, pp. 1301-1305, Oct, 2011.

[19] A. Shabaneh, S. Girei, P. Arasu *et al.*, "Dynamic Response of Tapered Optical Multimode Fiber Coated with Carbon Nanotubes for Ethanol Sensing Application," *Sensors*, vol. 15, no. 5, pp. 10452-10464, May, 2015.

[20] Q. Wang, G. Farrell, and W. Yan, "Investigation on single-mode-multimode single-mode fiber structure," *Journal Of Lightwave Technology*, vol. 26, no. 5-8, pp. 512-519, Mar-Apr, 2008.

[21] Q. Wang, and G. Farrell, "All-fiber multimode-interference-based refractometer sensor: proposal and design," *Optics Letters*, vol. 31, no. 3, pp. 317-319, Feb, 2006.

[22] A. Leung, P. M. Shankar, and R. Mutharasan, "A review of fiber-optic biosensors," *Sensors and Actuators B-Chemical*, vol. 125, no. 2, pp. 688-703, Aug, 2007.

[23] F. De-Jun, Z. Mao-Sen, G. X. Liu *et al.*, "D-Shaped Plastic Optical Fiber Sensor for Testing Refractive Index," *Ieee Sensors Journal*, vol. 14, no. 5, pp. 1673-1676, May, 2014.

[24] Q. Wu, Y. Semenova, B. B. Yan *et al.*, "Fiber refractometer based on a fiber Bragg grating and single-mode-multimode-single-mode fiber structure," *Optics Letters*, vol. 36, no. 12, pp. 2197-2199, Jun, 2011.

[25] J. Tang, J. Zhou, J. Guan *et al.*, "Fabrication of Side-Polished Single Mode-Multimode-Single Mode Fiber and Its Characteristics of Refractive Index Sensing," *IEEE Journal of Selected Topics in Quantum Electronics*, vol. 23, no. 2, pp. 1-8, 2017.

[26] J. Mathew, Y. Semenova, G. Rajan *et al.*, "Humidity sensor based on photonic crystal fibre interferometer," *Electronics letters*, vol. 46, no. 19, pp. 1341-1343, 2010.